

Study of the magnetic interaction of a 4-coil array and copper shielding with a PET/MRI using the finite-element method

S. E. Solís¹, D. Tomasi², and A. O. Rodriguez¹

¹Dep. Electrical Engineering, UAM Iztapalapa, Mexico, DF, Mexico, ²Medical Department, Brookhaven National Laboratory, Upton, NY, United States

Introduction. A single imaging modality cannot provide information on all aspects of structure and function. The combination of PET and MRI offers tantalizing opportunities, but also significant challenges. In particular, cross talk between the MRI transceiver and the PET digital electronics can lead to interfering RF noise in both imaging modalities. An electromagnetic shielding, decoupling the PET and MRI systems, must be tightly located between the RF coil of MRI and the PET scintillating crystals to minimize this interference without loosing space for the sample. Here we numerically studied the behaviour of a coil array with 4 squared-shaped elements for a PET-MRI system. The used of coil arrays is mainly motivated by the advantages offered by MRI parallel imaging.

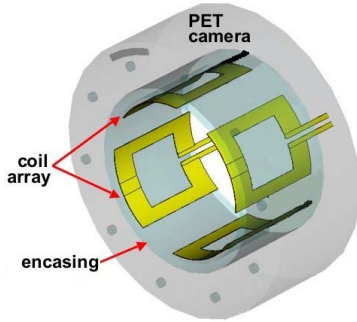


Fig. 1. PET-MRI setup with coil array

Method. The effect of the shielding in a PET-MRI system was numerically estimated by calculating the RF magnetic field, B_1 , produced by a coil array of 4 independent elements at the resonant frequency of 171 MHz (4T for protons). A finite element method (FEM) was used for this purpose. To numerically simulate the unshielded and shielded conditions, two- and three-dimensional FEM models were used assuming that coils were made out of copper. The RF coil array was surrounded with a cylinder that mimics the encasing of an existing PET camera [1], as indicated in Fig. 1. Simulations were performed using two different materials: copper ($\sigma=5.998 \times 10^7$ S/m & $\epsilon_r=1$) and aluminum ($\sigma=3.774 \times 10^7$ S/m & $\epsilon_r=1$). The thickness of the aluminum encasing was .2 mm. Numerical computation of the birdcage coil B_1 were also calculated for comparison purposes. All numerical computations were performed with the commercial software tool Comsol Multiphysics (COMSOL 3.2, Burlington, MA, USA), and the simulation parameters used for both cases and summarised in Table 1.

Results and discussion. The magnetic field produced by the 4-coil element array and 4-leg birdcage were simulated for the unshielded and shielded cases and assuming that the encasing was made of copper or aluminum. Fig. 2 shows the numerically calculated magnetic fields for all cases. Magnetic field uniformity profiles for all coils were also computed along the coil diameter for comparison purposes according to Fig. 3a). MATLAB programmes (Mathworks, 6.5, Natick, MA, USA) were specially written to compute the uniformity profiles and show in Fig. 2b)-c). A clear attenuation of the magnetic field produced by the birdcage coil can be appreciated in the exterior region produced by the aluminium and copper, see part *b* and *e*. Birdcage uniformity suffers a pretty similar decrement for both types of encasings. This is shown in part *c* of Fig. 2b)-c). The coil array shows the opposite effect, both the field uniformity and intensity increase moderately. This is probably due to a confinement of the field within the encasings (see right column of Fig. 2). The electromagnetic induction in the shielding marginally reduces the B_1 -field produced by the coil array (see part *a* and *d* in Fig. 3b)), and its uniformity experiences an improvement for both cases. The aluminium and copper encasings showed a similar attenuation of the magnetic field just outside protecting the delicate PET digital electronics from RF pulses. Unlike, the B_1 -field of the coil array is not efficiently attenuated by either of the encasings used in these simulations. This necessarily implies that a coil array requires of a thicker encasing. It still remains to investigate other type of materials to allow the use of coil array to take full advantage of the benefits of parallel imaging.

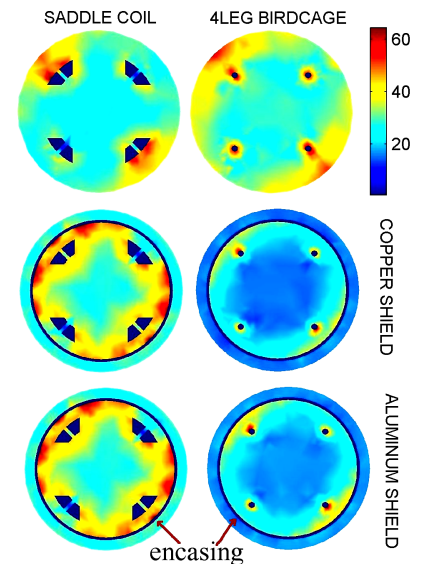


Fig. 2. Simulation of magnetic fields for the unshielded and the

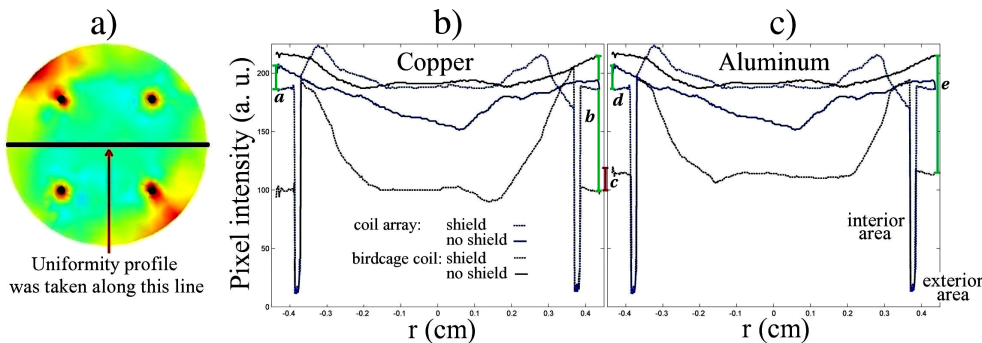


Fig. 3. a) Acquisition of comparison profiles. b) Uniformity profiles for two type of coils for two type of encasings, and the field attenuations are marked: *a*, *b*, *c*, *d*, and *e*.

References. [1] Woody C et. al NIM A 571:102,2007.